

electron's energy are not accounted for in the model. These would be expected to be larger for the smaller nuclei. A more detailed examination

of the formulation is required to see if one can retain the basic simplicity of the impulse model and obtain corrections for these effects.

\*Work supported in part by NASA Grant No. NGR 03-002-017, ONR Contract No. N00014-67-A-0209-0011 Project No. NR-000-111, and Aerospace Research Laboratories, Office of Aerospace Research, U. S. Air Force Contract No. F33615-70-C-1007. This manuscript is submitted for publication with the understanding that no limitation shall exist on the reproduction and distribution of its published or unpublished form in whole or in part for any purpose of the U. S. Government.

<sup>1</sup>J. D. Garcia, Phys. Rev. A 1, 280 (1970).

<sup>2</sup>J. D. Garcia, Phys. Rev. A 1, 1402 (1970).

<sup>3</sup>N. F. Mott and H. S. W. Massey, *The Theory of Atomic Collisions*, 3rd ed. (Oxford U. P., London,

1965), pp. 334-339; see also L. Vriens, *Physica* 47, 267 (1970).

<sup>4</sup>J. D. Garcia, E. Gerjuoy, and J. E. Welker, Phys. Rev. 165, 66 (1968).

<sup>5</sup>R. L. Watson, C. W. Lewis, and J. B. Natowitz, Nucl. Phys. A154, 561 (1970).

<sup>6</sup>N. L. Lark, Bull. Am. Phys. Soc. 7, 623 (1962).

<sup>7</sup>B. Sellers, F. A. Hanser, and H. H. Wilson, Phys. Rev. 182, 90 (1969).

<sup>8</sup>R. W. Fink, R. C. Jopson, H. Mark, and C. D. Swift, Rev. Mod. Phys. 38, 513 (1966).

<sup>9</sup>V. O. Kostroun, M. H. Chen, and B. Craseman, Phys. Rev. A 3, 533 (1971).

PHYSICAL REVIEW A

VOLUME 4, NUMBER 3

SEPTEMBER 1971

## Interpretation of Experimental Differential Elastic Scattering Cross Section for $H^+ + Ne^{\dagger}$

S. M. Bobbio, W. G. Rich, L. D. Doverspike, and R. L. Champion

*Department of Physics, College of William and Mary, Williamsburg, Virginia 23185*

(Received 15 March 1971)

The result of a differential scattering experiment of  $H^+$  by Ne at 5.71-eV collision energy is compared to the differential cross section predicted by (a) a JWKB partial-wave calculation based on a potential model, (b) a similar calculation based on the *ab initio* Peyerimhoff calculated intermolecular potential for the  $NeH^+$  system, and (c) a new and more efficient calculational scheme developed by Remler involving Regge poles. The agreement of the Peyerimhoff prediction, (b), with the experimental data is very good. Differences between the Peyerimhoff potential and the final values of the parameters retrieved from the iterative calculation in (a), as well as implicit ambiguities of (a) in reproducing the features of a low-resolution experiment, are discussed in terms of semiclassical theory and the Remler-Regge method.

### I. INTRODUCTION

The results and analysis of several experiments on the low-energy differential elastic scattering of  $H^+$  by noble-gas atoms have been reported.<sup>1</sup> In Ref. 1, the experimental differential cross section  $\sigma_{\text{exp}}(\theta)$  for each of the systems  $NeH^+$ ,  $ArH^+$ , and  $KrH^+$  was compared to a calculated differential cross section utilizing the JWKB method and a chosen analytic form for the interatomic potential  $V(r)$ . For each system the internuclear equilibrium separation  $r_m$  and the well depth  $U$  for the assumed  $V(r)$  were varied in the calculations until reasonable agreement was obtained between the experimental and calculated differential cross sections.

Since then we have come to believe that the results obtained from such potential-model calculations do not necessarily yield reliable intermolecular potentials, unless the resolution in the experiment is very good. The purpose of this paper is (a) to compare the  $V(r)$  found via the method de-

scribed above (and in Ref. 1) to an *ab initio* calculation of the intermolecular potential for  $NeH^+$  due to Peyerimhoff,<sup>2</sup> (b) to discuss why there is a rather significant difference in the two results, and (c) to apply a new method due to Remler<sup>3</sup> involving Regge poles which can be used to efficiently calculate the differential cross section, where the starting point for such calculations is based on one's intuition in light of the classical deflection function.

### II. EXPERIMENT AND SEMIQUANTAL CALCULATIONS

The semiquantal calculation of Ref. 1 as regards the  $NeH^+$  system will be briefly recapitulated. The JWKB phase shifts were found using the potential model

$$V(r) = (\tilde{C}/\rho) \exp\beta(1 - \rho) - C_6/\rho^6 - C_4/\rho^4, \quad (1)$$

with

$$\rho = r/r_m, \quad C_4 = \alpha e^2/2r_m^4,$$

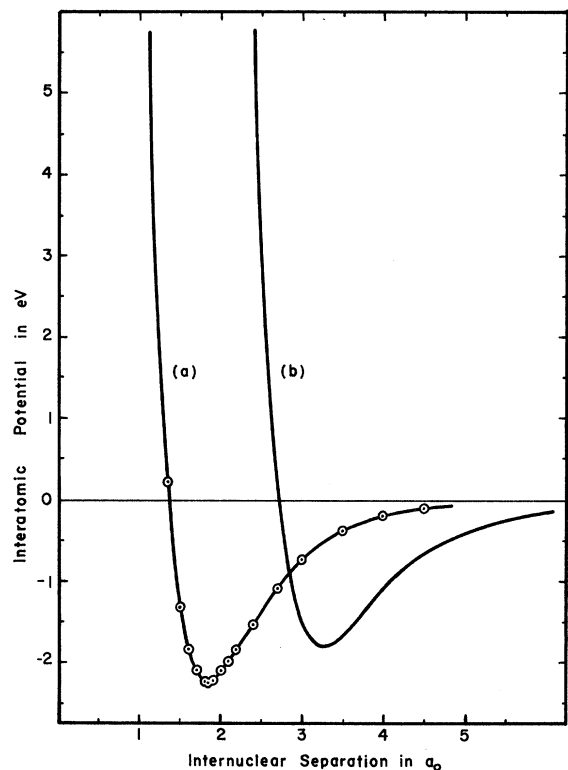


FIG. 1. Intermolecular potentials for the  $\text{NeH}^+$  system: (a) Peyerimhoff calculated points and analytic fit; (b) potential model.

$$C = C_6 + C_4 - U, \quad \beta = (6C_6 + 4C_4)/C - 1,$$

where  $r_m$  is the position of the potential minimum,  $U$  is the depth of the potential well, and  $\alpha$  is the dipole polarizability of the target atom. The differential cross section  $\sigma_{\text{mod}}(\theta)$ , calculated by using these phase shifts in the Rayleigh-Faxen-Holtzmark (RFH) partial-wave sum, was brought into satisfactory agreement with the data by varying the parameters  $r_m$ ,  $U$ , and  $C_6$ . This procedure was applied to the system  $\text{NeH}^+$  and no attempt was made to reproduce the high-frequency oscillations seen in the 5.71-eV experiment<sup>4</sup> shown in Fig. 2(c). The values of the potential parameters necessary to achieve a satisfactory fit to the low-frequency oscillations in the data were  $r_m = 3.25a_0$ ,  $U = 1.8$  eV, and  $C_6 = 5.0$  eV. This potential is shown in Fig. 1(b).

The differential cross section  $\sigma_{\text{mod}}(\theta)$ , calculated (at 5.71 eV) on the basis of the potential model of Ref. 1, is shown as a dashed line in Fig. 2(d). The heavy black line superimposed on the dashed line is the result of a convolution of the calculation with a function whose width is thought to be representative of the experimental resolution. It is clear that, even though the large (i.e., low-frequency)

oscillations of  $\sigma_{\text{expt}}(\theta)$  in Fig. 2(c) are in good agreement with those of  $\sigma_{\text{mod}}(\theta)$  in Fig. 2(d), the fine oscillations in the calculation have a much higher frequency than those in the data. It shall be shown in Secs. III and IV that the experimental resolution of these high-frequency oscillations and the necessity to reproduce them in the calculation place important restrictions on the intermolecular potential.

It is of interest to compare the calculated differential cross section, utilizing the potential discussed above, with the differential cross section predicted by an *ab initio* pointwise calculated intermolecular potential of Peyerimhoff<sup>2</sup> for the system  $\text{NeH}^+$ . An analytic function has been fitted to the points of the Peyerimhoff potential [shown in Fig. 1(a)] and used in a standard JWKB calculation for the phase shifts.

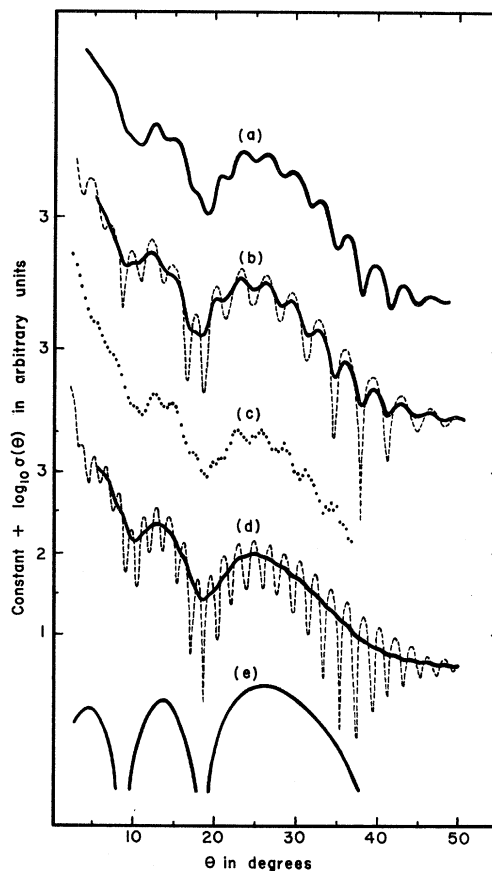


FIG. 2. Logarithm of the relative elastic differential cross section vs c.m. scattering angle for  $\text{H}^+ + \text{Ne}$  at 5.71-eV collision energy: (a) Remler-Regge calculation with only the convolution displayed; (b) dashed line—semiquantal calculation made using Peyerimhoff potential, solid line—convolution of dashed line; (c) experimental observation; (d) dashed line—semiquantal calculation made using potential model, solid line—convolution of dashed line; (e) low-frequency oscillations predicted by semiclassical rainbow scattering theory.

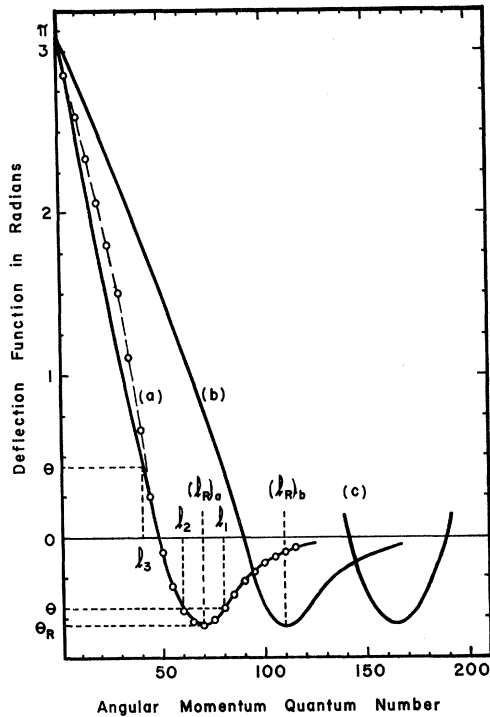


FIG. 3. Deflection functions for the  $H^+ + Ne$  system at 5.71-eV collision energy: (a) circles with dashed line—points on the deflection function predicted by the Remler-Regge method, solid line—prediction of the Peyerimhoff potential; (b) prediction of the potential model; (c) parabola whose curvature fits the attractive portion of both 3(a) and 3(b).

These phase shifts have been used in the RFH sum over partial waves to find the differential cross section  $\sigma_{\text{Pey}}(\theta)$ , shown in Fig. 2(b).

The agreement between  $\sigma_{\text{Pey}}(\theta)$ , Fig. 2(b), and  $\sigma_{\text{exp}}(\theta)$ , Fig. 2(c), is very good regarding both the high- and low-frequency oscillations. The largest difference between  $\sigma_{\text{Pey}}(\theta)$  and  $\sigma_{\text{exp}}(\theta)$  is a small (about  $1^\circ$ ) discrepancy in the positions of the low-frequency oscillations. It should be pointed out that the value of  $U$  (2.21 eV) from the Peyerimhoff calculation is in good agreement with the experimental measurement (2.29 eV) reported by Chupka and Russel.<sup>5</sup>

The two potentials presented in Fig. 1 are clearly very dissimilar, and yet both predict the periodicity of the large oscillations in the experimental differential cross section. It shall be shown in Sec. III why both of these potentials lead to the same differential cross section in the limit of low angular resolution.

### III. SEMICLASSICAL INTERPRETATION

The potentials in Figs. 1(a) and 1(b) lead to the corresponding deflection functions shown by solid

lines in Figs. 3(a) and 3(b). The deflection function  $\Theta$  is related to the potential by

$$\Theta(l) = \pi - \frac{2}{k} \left( l + \frac{1}{2} \right)$$

$$\int_{r_0}^{\infty} r^{-2} \left[ dr / \left( 1 - \frac{V(r)}{E} - \frac{(l + \frac{1}{2})^2}{k^2 r^2} \right)^{1/2} \right] \quad (2)$$

(where  $k$  is the wave number,  $E$  is the collision energy, and  $r_0$  is the classical turning point), to the JWKB phase shift  $\eta$  by

$$\frac{\partial \eta(l)}{\partial l} = \frac{1}{2} \Theta(l), \quad (3)$$

and to the c. m. scattering angle by

$$\begin{aligned} \theta &= -\Theta \quad \text{for attractive scattering} \\ &= +\Theta \quad \text{for repulsive scattering.} \end{aligned} \quad (4)$$

In the semiclassical framework oscillations in the differential cross section for  $\theta$  less than or equal to the attractive scattering maximum  $\theta_{\text{rainbow}}$  (hereafter labeled  $\theta_R$ ) are due to the interference of three partial waves having  $l = l_1, l_2, l_3$  as labeled in Fig. 3(a). For  $\theta > \theta_R$ , only the repulsive branch of the deflection function contributes to the differential cross section. Clearly the attractive branches of both deflection functions [Figs. 3(a) and 3(b)] are very similar. The obvious difference in the two curves is the value of  $l_{\text{rainbow}}$  (hereafter labeled  $l_R$ ), which is the angular momentum quantum number corresponding to  $\Theta_R$  for a given collision energy.

The first successful attempt to predict the differential cross section in terms of semiclassical theory was made by Ford and Wheeler.<sup>6</sup> In their work the deflection function in the vicinity of  $\Theta_R$  was fitted to a parabola of the form

$$\Theta(l) = \Theta_R + q(l - l_R)^2, \quad (5a)$$

$$q = \frac{1}{2} \left( \frac{\partial^2 \Theta}{\partial l^2} \right)_{l=l_R}, \quad (5b)$$

the resulting differential cross section being<sup>7</sup>

$$\sigma(\theta) = \sigma_c(\theta) + \sigma_R(\theta) + 2[\sigma_c(\theta) \sigma_R(\theta)]^{1/2} \cos(\delta - \gamma_c), \quad (6a)$$

with

$$\sigma_c(\theta) = -l_c / k^2 \left( \frac{\partial \theta}{\partial l} \right)_{l_c} \sin \theta, \quad (6b)$$

$$\sigma_R(\theta) = (2\pi l_R / k^2 \sin \theta) q^{-2/3} \text{Ai}^2(q^{-1/3}(\theta - \theta_R)),$$

where  $l_c$  is the angular momentum quantum number corresponding to the contribution from the repulsive part of the deflection function to the scattering at  $\theta_R$ , and

$$\delta = 2\eta(l_R) + l_R \theta - \frac{3}{4} \pi, \quad \gamma_c = 2\eta(l_c) - l_c(\theta) - \frac{1}{2} \pi. \quad (6c)$$

The low-frequency oscillations observed in the differential cross section are due to the term that contains the square of the Airy function. The argument of the Airy function,  $q^{-1/3}(\theta - \theta_R)$ , does not depend upon  $l_R$ , but is a function of  $\theta_R$  and the curvature  $q$  of the parabola. Figure 3(c) is a parabola with  $q = 10^{-3}$  rad whose curvature fits the attractive portion of both Figs. 3(a) and 3(b) equally well (for clarity, this parabola is shown displaced to the right of the deflection functions in Fig. 3). The Airy function corresponding to the  $q$  is plotted in Fig. 2(e). Note that if  $\theta_R$  is fixed and the attractive portion of the deflection function is made wider, the curvature  $q$  is thereby decreased, and, as is seen via Eq. (6b), the number of low-frequency oscillations predicted in the differential cross section increases. Thus it is possible to change the periodicity of the low-frequency oscillations in the calculated differential cross section by changing the curvature of the attractive portion of the deflection function. The low-frequency oscillations in the differential cross sections of Figs. 2(b), 2(c), and 2(d) have the same periodicity as the square of the Airy function shown in Fig. 2(e). This agreement clearly demonstrates that in the semiclassical approximation the low-frequency oscillations in the differential cross section around the rainbow angle are dependent upon the shape and the depth of the attractive portion of the deflection function, and in *no* way depend upon the location of  $l_R$ . Thus all potentials which lead to deflection functions whose attractive branches are of the same shape and depth, but differ in  $l_R$ , will predict equally well the periodicity of the low-frequency oscillations in the relative differential cross section in the region of the rainbow angle.

The argument of the cosine term in Eq. (6a),

$$\delta - \gamma_c = (l_R + l_c)\theta + 2[\eta(l_R) - \eta(l_c)] - \frac{1}{4}\pi, \quad (7)$$

is responsible for the high-frequency oscillations in the differential cross section. Therefore the frequency of these oscillations is proportional to  $l_R + l_c$ . Since  $(l_R)_a < (l_R)_b$  in Fig. 3, it is not surprising that the fine oscillations of the differential cross section in Fig. 2(d) have a higher frequency than those of the differential cross section in Fig. 2(b). Thus the experimental resolution of the fine oscillations in the differential cross section enables one to locate the minimum of the deflection function and consequently the corresponding intermolecular potential may be more accurately determined.

In some cases, two of which are discussed below, the value of  $l_R$  can be found without knowing the periodicity of the high-frequency oscillations. It has been pointed out<sup>8</sup> that if absolute differential cross-section measurements are made, the value of  $l_R$  can in principle be determined. This is due to the fact that the scattered intensity at the rain-

bow angle is proportional to the corresponding impact parameter and hence proportional to  $l_R$ . Another method of obtaining a value of  $l_R$  is to experimentally observe equally spaced low-frequency oscillations at small ( $< 30^\circ$ ) angles which may be attributed to "glory" scattering.<sup>9</sup> The periodicity of such oscillations can be directly related to  $l_0$ , the  $l$  value for which  $\Theta(l)$  passes continuously through zero. From the experimental determination of the position of  $l_0$  and a knowledge of  $q$ , the curvature of the deflection function around  $\Theta_R$ , the value of  $l_R$  may then be inferred. However, since  $\sigma_{\text{expt}}(\theta)$  in Fig. 2(c) for the NeH<sup>+</sup> system at 5.71 eV does not show sufficiently detailed "glory" structure, the procedure just outlined cannot be applied in this case.

#### IV. REMLER-REGGE METHOD

The semiclassical arguments of Sec. III are appealing because of their simplicity, but they are strictly valid only for scattering in the region of the rainbow angle. A recent theoretical treatment developed by Remler<sup>3</sup> will allow the extension of the results of Sec. III to a larger range of  $\theta$ .

A brief discussion of the Remler treatment is in order. It is not our purpose, however, to develop the subject in detail, and the interested reader should consult Ref. 3 for a deeper understanding. Regge<sup>10-12</sup> has shown that the infinite sum over partial waves for the scattering amplitude may, in certain cases, be replaced by a finite sum over singularities of the  $S$  matrix in the complex angular momentum plane. Remler<sup>3</sup> has parametrized the  $S$ -matrix elements in such a way that the resulting singularities may be directly related to the classical deflection function. In practice, a number of poles  $N$  are positioned on a circle centered at some point  $L_p$  in the first quadrant of the angular momentum plane. The circular placement of the poles is advantageous in that it allows all the poles to be treated in the calculation as if they had been placed at  $L_p$ . The three parameters [ $N$ ,  $\text{Re}(L_p)$ , and  $\text{Im}(L_p)$ ] are sufficient to determine the periodicity as well as the location of *both* the low- and high-frequency oscillations observed in the calculated differential cross section.

The simplicity of applying this treatment is very appealing. The rainbow angle is given approximately by

$$\theta_R = 2N/\text{Im}(L_p). \quad (8)$$

For fixed  $\theta_R$  the number of low-frequency oscillations increase as  $N$  is increased, since the width of the attractive portion of the corresponding deflection function is proportional to  $2\text{Im}(L_p)$ . The frequency of the fine oscillations in this treatment is completely decoupled from the parameters  $N$  and

$\text{Im}(L_p)$ . In fact, the frequency of the fine oscillations is directly proportional to  $\text{Re}(L_p)$ , which in semiclassical terms is equal to  $l_R$  (the location of the minimum of the deflection function). Since both high- and low-frequency components may be varied independently in the calculation, this method proves to be a flexible and efficient scheme to reproduce the features of the experimentally observed cross section.

The convolution of the differential cross section resulting from a Remler-Regge calculation with parameters  $\text{Re}(L_p)=70$ ,  $\text{Im}(L_p)=21.88$ , and  $N=6$  is plotted in Fig. 2(a); a number of points on the corresponding deflection function are shown as circles connected by a dashed line in Fig. 3(a). The Remler-Regge cross section is in good agreement with both  $\sigma_{\text{expt}}(\theta)$  in Fig. 2(c) and  $\sigma_{\text{Pey}}$  in Fig. 2(b).

The positions of the low-frequency oscillations do not depend upon  $\text{Re}(L_p)$ . In fact, the value of  $\text{Re}(L_p)$  was varied from 50 to 250 with absolutely no effect on their location at any angle. Thus the lack of dependence of these oscillations on  $l_R$  pointed out in Sec. III is further supported.

#### V. CONCLUSION

The discussions in Secs. III and IV serve to point out that the relative differential cross sections measured in low-resolution experiments do not unambiguously determine the intermolecular potential. In fact, there exist many intermolecular potentials which correspond to deflection functions

whose attractive portions differ only in  $l_R$ , and all of which predict the periodicity of the observed low-frequency oscillations. Thus care must be exercised in applying a potential-model treatment to differential scattering data. Furthermore, the values of potential parameters retrieved from such calculations are subject to uncertainty when the high-frequency component of the differential cross section has not been resolved experimentally.

The Remler-Regge method of calculating the differential cross section proves to be much more efficient than the standard semiquantal method in that it replaces the infinite partial-wave sum by a finite (six terms in the  $\text{NeH}^+$  case) sum over singularities of the  $S$ -matrix elements in the complex angular momentum plane. More importantly, however, the mathematical form of these  $S$ -matrix elements allows them to be simply and directly connected to the classical deflection function. This connection with the deflection function is useful in that semiclassical intuition may be applied effectively to the analysis of a given scattering experiment. Moreover, the deflection function retrieved from the Remler-Regge calculation could serve as a starting point for an inversion procedure to find the intermolecular potential.

#### ACKNOWLEDGMENT

We would like to thank Professor E. A. Remler for many valuable discussions as well as for the basic computer program utilized in Sec. IV.

<sup>†</sup>Supported in part by the National Science Foundation.

<sup>1</sup>R. L. Champion, L. D. Doverspike, W. G. Rich, and S. M. Bobbio, *Phys. Rev. A* **2**, 2327 (1970).

<sup>2</sup>S. Peyerimhoff, *J. Chem. Phys.* **43**, 998 (1965).

<sup>3</sup>E. A. Remler, *Phys. Rev. A* **3**, 1949 (1971).

<sup>4</sup>This energy was erroneously labeled 6 eV in Sec. IV B of Ref. 1.

<sup>5</sup>W. A. Chupka and M. E. Russel, *J. Chem. Phys.* **49**, 5426 (1968).

<sup>6</sup>K. W. Ford and J. A. Wheeler, *Ann. Phys. (N. Y.)* **7**, 259 (1959); **7**, 287 (1959).

<sup>7</sup>R. B. Bernstein, in *Advances in Chemical Physics*, edited by John Ross (Interscience, New York, 1966), Vol. X, pp. 103, 104.

<sup>8</sup>F. A. Herrero, E. M. Nemeth, S. J., and T. L. Bailey, *J. Chem. Phys.* **50**, 4591 (1969).

<sup>9</sup>R. E. Olson, *J. Chem. Phys.* **49**, 4499 (1968).

<sup>10</sup>T. Regge, *Nuovo Cimento* **14**, 951 (1959).

<sup>11</sup>A. Bottino, A. M. Langoni, and T. Regge, *Nuovo Cimento* **23**, 954 (1962).

<sup>12</sup>V. DeAlfaro and T. Regge, *Potential Scattering* (Wiley, New York, 1965).